

Vision-Language Reasoning for Geolocalization: A Reinforcement Learning Approach

Biao Wu¹, Meng Fang², Ling Chen¹, Ke Xu², Tao Cheng³, Jun Wang³

¹University of Technology Sydney, Australia

²University of Liverpool, United Kingdom

³University College London, United Kingdom

biao.wu-2@student.uts.edu.au, Meng.Fang@liverpool.ac.uk, Ling.Chen@uts.edu.au,
Ke.Xu@liverpool.ac.uk, tao.cheng@ucl.ac.uk, jun.wang@ucl.ac.uk

Abstract

Recent advances in vision-language models have opened up new possibilities for reasoning-driven image geolocalization. However, existing approaches often rely on synthetic reasoning annotations or external image retrieval, which can limit interpretability and generalizability. In this paper, we present Geo-R, a retrieval-free framework that uncovers structured reasoning paths from existing ground-truth coordinates and optimizes geolocation accuracy via reinforcement learning. We propose the Chain of Region, a rule-based hierarchical reasoning paradigm that generates precise, interpretable supervision by mapping GPS coordinates to geographic entities (e.g., country, province, city) without relying on model-generated or synthetic labels. Building on this, we introduce a lightweight reinforcement learning strategy with coordinate-aligned rewards based on Haversine distance, enabling the model to refine predictions through spatially meaningful feedback. Our approach bridges structured geographic reasoning with direct spatial supervision, yielding improved localization accuracy, stronger generalization, and more transparent inference. Experimental results across multiple benchmarks confirm the effectiveness of Geo-R, establishing a new retrieval-free paradigm for scalable and interpretable image geolocalization. To facilitate further research and ensure reproducibility, all relevant resources, including the model and code, are publicly available at <https://github.com/ailt/geo-r>.

1 Introduction

Image geolocalization—the task of predicting the geographic coordinates of an image—poses unique difficulties, particularly at the global scale. The inherent difficulty of this task arises from the high diversity of geographic regions, the visual similarity between distant locations, and the lack of explicit geographic cues in many images. Existing methods mainly fall into two categories: classification-based approaches, which partition the Earth into discrete regions and treat geolocation as a classification task (Weyand, Kostrikov, and Philbin 2016; Seo et al. 2018a; Müller-Budack, Pustu-Iren, and Ewerth 2018; Pramanick et al. 2022a; Clark et al. 2023a), and retrieval-based approaches, which retrieve the most visually similar samples from large-scale geo-tagged image databases (Yang, Lu, and Zhu 2021; Zhu, Shah, and Chen 2022; Wang et al. 2023; Vivanco Cepeda, Nayak, and Shah 2023; Haas et al. 2024; Xia and Alahi 2025;

Haas, Alberti, and Skreta 2023). While both paradigms have achieved strong benchmark performance, they rely heavily on large-scale labeled data or retrieval databases and often lack interpretability and robust reasoning capabilities, limiting their generalization to unseen regions.

Reasoning for geolocalization is challenging and less studied, as it requires models to generate interpretable, structured explanations that align with visual evidence—a task further complicated by the scarcity of annotated reasoning paths. While recent advances in vision-language modeling have driven progress in related areas such as visual recognition, language grounding, and cross-modal retrieval (Chen et al. 2023; Koh, Salakhutdinov, and Fried 2023; Wang et al. 2025a; Wu et al. 2024), there is still little work addressing geolocalization using vision-language models (VLMs). Techniques such as few-shot prompting, retrieval-augmented generation (RAG), and supervised fine-tuning (SFT) (Jia et al. 2024; Zhou et al. 2024) allow models to produce both geolocation predictions and their corresponding reasoning processes. However, these methods typically rely on synthetic data to construct structured reasoning annotations, which only partially addresses the lack of real-world annotated data. Synthetic supervision frequently results in shallow or inconsistent reasoning that may not accurately reflect the visual evidence, thus constraining overall model performance.

To address these challenges, we propose Geo-R, a retrieval-free, reasoning-centric model for global image geolocalization built on the Geo Chain-of-Thoughts (CoT) paradigm. Geo-R mimics human geographic reasoning by progressively localizing an image from country to state to city, and finally estimating its precise coordinates. By clearly labeling each geographic level, this hierarchical approach decomposes the complex geolocation task into a sequence of interpretable subgoals, reducing the difficulty of direct coordinate regression and explicitly leveraging the latent geographic priors embedded in vision-language models (VLMs), thereby improving both accuracy and interpretability. Meanwhile, we construct MP16-Rand-500K, a large-scale, high-quality geographic reasoning dataset covering diverse global locations. Its reasoning sequences are generated by reverse-decoding ground-truth coordinates into multi-level geographic information, producing a coherent coarse-to-fine structure aligned with the hierarchical pre-

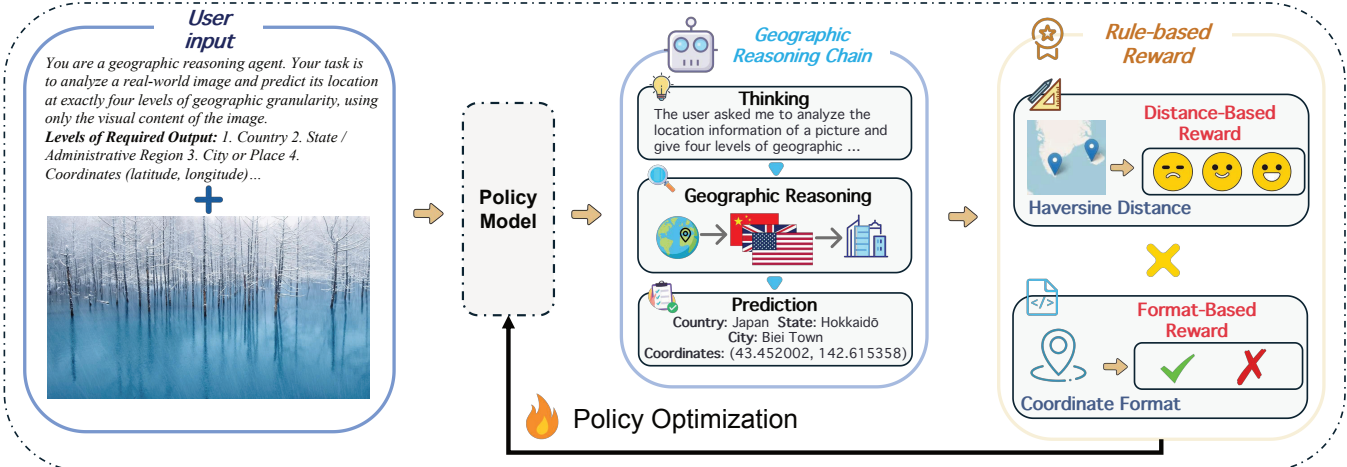


Figure 1: Overview of Geo-R for image geolocation. Given a query image, the agent generates a region-level reasoning chain grounded in geographic knowledge, followed by coordinate prediction. The framework integrates structured prompting, multi-modal understanding, and reinforcement optimization to enhance both interpretability and spatial accuracy.

diction process of Geo-R. This dataset is employed in the SFT stage to further enhance the model’s structured geographic reasoning ability, laying a solid foundation for more advanced training and evaluation.

Furthermore, we observe that the core evaluation metric in geolocation tasks is the proximity of predicted coordinates to the ground truth. However, in regression tasks, SFT usually does not penalize small numerical errors, making it difficult to improve prediction accuracy directly. In contrast, Reinforcement Learning (RL) provides continuous and directional optimization signals for numerical errors—for example, assigning higher rewards as predicted coordinates approach the ground truth. Based on this insight, we introduce an RL stage and optimize the model within the Group Relative Policy Optimization (GRPO) (Shao et al. 2024), using a composite reward function that jointly accounts for spatial accuracy and faithful reasoning. However, during training, we identify a critical issue with GRPO: the vanishing advantages problem. When all responses within a query group receive identical rewards (e.g., all correct or all incorrect), the computed relative advantages approach zero, resulting in ineffective gradient updates. This issue is especially pronounced in later training stages, where a large portion of samples originate from “popular regions” such as city centers or iconic landmarks. These regions often exhibit salient visual cues and low localization difficulty, leading to uniform predictions and reward saturation—ultimately limiting the model’s capacity to generalize to more complex scenarios. To mitigate this, we introduce a diversity-based data filtering mechanism and construct a more challenging subset, MP16-Hard-200K, by excluding all samples within a 200-kilometer radius of popular regions and focusing instead on remote, visually ambiguous, or culturally neutral areas. These long-tailed and difficult examples significantly enhance training diversity and reward signal variance, effectively alleviating the vanishing advantages problem and further improving the model’s generalization and reason-

ing performance in complex, real-world geographic environments.

We conduct comprehensive evaluations of Geo-R on two standard geolocation benchmarks. Experimental results demonstrate that our method achieves strong performance across both coarse-grained tasks at the country levels and fine-grained tasks at the regional level. Compared to retrieval-based baselines, Geo-R not only delivers competitive localization accuracy but also provides superior interpretability, cross-domain generalization, and robustness across a wide range of geographic conditions. These findings validate the feasibility and effectiveness of a retrieval-free, reasoning-driven paradigm for geolocation and point toward a new direction for building scalable and general-purpose geographic agents.

Our key contributions are fourfold:

- We introduce Geo-R, a retrieval-free, reasoning-driven architecture for global image geolocation.
- We propose the geo Chain-of-Thoughts paradigm and accompany it with a scalable data-synthesis pipeline and richly annotated geographic-reasoning dataset, enabling the model to learn structured, hierarchical inference from visual cues.
- We develop a novel reinforcement-learning framework with plausibility rewards, directly optimizing geographic accuracy via spatial-distance-based signals while enforcing strict output formatting.
- Our experiments demonstrate that pure reasoning—without any external retrieval—can match or surpass traditional retrieval-based pipelines in both localization accuracy and cross-domain generalization across diverse global environments.

2 Related Work

2.1 Image Geolocalization

Image geo-localization aims to predict the geographic coordinates of a given image and has wide applications in urban analysis (Yeh 1999; Firmansyah et al. 2024; Yan et al. 2024; Ye et al. 2019a,b), navigation (DeSouza and Kak 2002), and geospatial data mining (Körting, Fonseca, and Câmara 2013; Liu et al. 2024; Liang et al. 2018; Pan et al. 2019; Hao et al. 2025). With the rapid progress of multimodal learning, the research paradigm for image geo-localization has gradually shifted from traditional classification-based methods (Weyand, Kostrikov, and Philbin 2016; Seo et al. 2018a; Müller-Budack, Pustu-Iren, and Ewerth 2018; Pramanick et al. 2022a; Clark et al. 2023a) and retrieval-based pipelines (Yang, Lu, and Zhu 2021; Zhu, Shah, and Chen 2022; Wang et al. 2023; Vivanco Cepeda, Nayak, and Shah 2023; Xia and Alahi 2025; Haas, Alberti, and Skreta 2023) to generation-based reasoning approaches (Zhou et al. 2024; Jia et al. 2024) that offer better interpretability and generalization. These methods utilize vision-language models (VLMs) to produce structured reasoning paths and coordinate predictions. Recent work has proposed synthetic reasoning datasets constructed by distilling reasoning capabilities from multiple VLMs, yielding annotations such as locatability assessments, reasoning trajectories, and predicted coordinates. Based on this, models are further optimized using Group Relative Policy Optimization (GRPO), significantly improving interpretability and geographic accuracy. However, such approaches still rely on distilled synthetic reasoning data, which may suffer from hallucinations, redundancy, or structural inconsistency. To address these limitations, we propose Geo-R, a truly retrieval-free and distillation-free reasoning-centric framework that effectively integrates structured reasoning supervision with coordinate-level optimization objectives, thereby enhancing both semantic interpretability and geographic precision with improved robustness.

2.2 Verifiable Rewards for VLMs

Recent advances in multimodal learning have sparked growing interest in using reinforcement learning with verifiable rewards to enhance the reasoning capabilities of VLMs. A series of studies have shown that R1-guided training can promote structured inference: R1-OneVision (Yang et al. 2025), Infinity Parserv (Wang et al. 2025a) create visual reasoning datasets by translating images into textual form and apply reward-driven fine-tuning to improve interpretability. R1-V (Chen et al. 2025) adopts GRPO (Shao et al. 2024), introduced in DeepSeek R1 (Guo et al. 2025), to outperform much larger models in object-counting tasks. Additional work such as VisualThinker-R1-Zero (Zhou et al. 2025) and VI-Rethinker (Wang et al. 2025b) reveals emergent reasoning abilities like the “visual aha moment” through R1 and (Kool, van Hoof, and Welling 2019). Other directions include curriculum-based reward strategies (Deng et al. 2025) and joint text-multimodal RL training (LMM-R1 (Peng et al. 2025)). While most of these efforts focus on mathematical reasoning (Lu et al. 2023), works like Visual-RFT (Liu et al.

2025) begin to explore perceptual reasoning. In contrast, we apply GRPO to spatial reasoning with retrieval-free supervision, directly optimizing coordinates with geographic plausibility rewards to achieve accurate and interpretable geolocalization.

3 Methodology

In this section, we present Geo-R, a reasoning-centric and retrieval-free framework for global image geolocalization that bridges symbolic reasoning and spatial precision. Geo-R enables VLMs to infer geographic locations through structured, interpretable, and verifiable reasoning chains. The framework comprises three key components: (1) Chain-of-Region (CoR), a reasoning paradigm that guides the model to infer hierarchical geographic labels based on visual cues; (2) a reinforcement learning stage optimized under the GRPO framework, which uses a composite reward to jointly improve coordinate accuracy and format consistency; and (3) a diversity-driven data selection strategy, which constructs a challenging subset from visually ambiguous and underrepresented regions to enhance generalization.

3.1 Synthesizing Geographic Reasoning Data at Scale

To effectively activate the latent geographic knowledge and spatial reasoning capabilities of VLMs, we propose CoR, a structured reasoning paradigm that reformulates image geolocalization as a step-by-step inferential process. While VLMs possess extensive world knowledge and cross-modal understanding, we observe that directly regressing geographic coordinates often fails to elicit deeper geographic cognition. In contrast, VLMs are inherently better suited for structured reasoning, hierarchical decision-making, and language-driven inference chains. Our CoR addresses this by guiding the model to generate spatial judgments based on visible cues in the image—such as landmarks, vegetation, architectural styles, and climate—thereby enabling a reasoning transition from what is seen to where it is.

To support this paradigm at scale, we design a data synthesis pipeline that automatically generates richly annotated samples for geographic reasoning. A key insight is that each reasoning label—country, region, city—can be automatically derived by reverse-decoding the ground-truth coordinates using global administrative boundary databases and geocoding tools. This removes the need for manual annotation while aligning perfectly with our CoR output format. In total, we synthesize 500K geographically diverse reasoning samples, denoted as MP16-Rand-500k, forming a solid foundation for training VLMs to reason about place with precision and structure.

3.2 Reinforcement Learning for Geographic Reasoning

To enable reinforcement learning with verifiable rewards for geographic reasoning, we adopt GRPO as our training framework (Shao et al. 2024). Unlike traditional methods that evaluate each output in isolation, GRPO compares multiple candidate responses generated from the same input

to estimate their relative advantages, enabling group-wise ranking to guide stable and informed policy updates. To support this framework and better align with the characteristics of geographic reasoning, we design a composite reward function that jointly captures both spatial precision and format consistency. Specifically, we incorporate two complementary components: a distance-based reward, which uses Haversine distance to measure the geodesic error between the predicted and ground-truth coordinates—encouraging geographically accurate and directionally reasonable predictions—and a format-based reward, which assigns a positive score only when the model output includes a single, well-structured, and parsable latitude-longitude pair. By combining these two components, the reward function ensures that only predictions which are both accurate and interpretable contribute to policy optimization, thereby providing fine-grained, verifiable learning signals well-suited to the demands of geographic reasoning.

Distance-Based Reward The first component of our reward function measures the spatial accuracy of the predicted coordinates (x_1, y_1) against the ground-truth coordinates (x_2, y_2) using the Haversine distance (Sinnott 1984), which accounts for the curvature of the Earth. Let $R = 6371$ km denote the Earth’s mean radius.

We first compute the differences in latitude and longitude (in radians) between the predicted and actual locations:

$$\Delta x = x_2 - x_1, \quad \Delta y = y_2 - y_1 \quad (1)$$

where Δx is the north–south angular difference and Δy is the east–west angular difference. Next, we calculate the intermediate term a , which corresponds to the squared half-chord length between the two points on the unit sphere:

$$a = \sin^2\left(\frac{\Delta x}{2}\right) + \cos(x_1) \cdot \cos(x_2) \cdot \sin^2\left(\frac{\Delta y}{2}\right) \quad (2)$$

This term combines the north–south and east–west components while considering the Earth’s curvature. We then obtain the central angle c between the two points, and multiply by R to get the great-circle distance d in kilometers:

$$c = 2 \cdot \arcsin(\sqrt{a}), \quad (3)$$

$$d = R \cdot c. \quad (4)$$

Here, d represents the shortest distance over the Earth’s surface between the predicted and actual locations. Finally, the distance-based reward r_{distance} is defined as a piecewise function of d , decreasing smoothly as d increases and capped at 20000 km (the approximate maximum great-circle distance between two antipodal points, $\pi R \approx 20000$ km):

$$r_{\text{distance}} = \begin{cases} 1.0 - 0.5 \cdot \frac{d}{750}, & d \leq 750, \\ 0.5 - 0.3 \cdot \frac{d-750}{1750}, & 750 < d \leq 2500, \\ 0.2 - 0.2 \cdot \frac{d-2500}{17500}, & \text{otherwise.} \end{cases} \quad (5)$$

This reward structure ensures high rewards for precise predictions, moderate penalties for mid-range errors, and gradual decay for very distant predictions, thereby maintaining informative gradient signals even for large errors.

Format-Based Reward Models often exhibit *format hallucinations*, producing outputs with missing coordinates, multiple ambiguous candidates, or inconsistent placement, which hinders downstream evaluation. To address this, we define a binary format reward that assigns 1 only when the output contains exactly one valid decimal latitude–longitude pair in the expected form—enclosed in parentheses and separated by a comma; otherwise, it assigns 0. This encourages strict adherence to the output template, penalizes ambiguous or ill-structured predictions, and, when combined with the distance-based reward, ensures contributions come only from accurate and well-formatted predictions.

$$r_{\text{format}} = \begin{cases} 1, & \text{valid coordinate pair in expected format,} \\ 0, & \text{otherwise.} \end{cases} \quad (6)$$

The overall reward r for a single sample combines both components:

$$r = r_{\text{distance}} \times r_{\text{format}}, \quad (7)$$

where r_{distance} captures the spatial precision of the prediction, and r_{format} reflects the semantic alignment and interpretability of the reasoning chain. The total reward serves as the training signal in the reinforcement learning phase.

3.3 Diverse Geographic Reasoning Data Selection

To enhance the model’s generalization ability across diverse and geographically challenging scenarios, we construct a hard subset from the MP16-Pro (Jia et al. 2024) dataset, denoted as MP16-Hard-200k. Specifically, we first identify 100k MP16-Pro (Jia et al. 2024) samples that Qwen-VL-3B (Bai et al. 2025) localizes correctly; these samples form dense spatial clusters concentrated around major population centers and iconic landmarks—regions we term “popular regions” due to the model’s likely prior exposure or access to strong visual cues. To extract more challenging cases, we exclude all samples located within a 200-kilometer radius of any such popular region. The remaining samples, typically drawn from remote, visually ambiguous, or culturally neutral areas, compose the MP16-Hard-200k subset. These examples present greater localization difficulty and are used to augment model training, encouraging stronger spatial reasoning in underrepresented geographies. This targeted selection approach serves as a practical means of pushing models beyond surface-level pattern recognition, promoting robust geospatial understanding under real-world, long-tail conditions.

4 Experiments

4.1 Datasets

Training Data We primarily use two datasets—MP16-Rand-500K and MP16-Hard-200K—both constructed from

Methods	IM2GPS3K						YFCC4K					
	1km	25km	200km	750km	2500km		1km	25km	200km	750km	2500km	
<i>Retrieval-based Methods</i>												
[L]kNN, $\sigma = 4$	ICCV'17	7.2	19.4	26.9	38.9	55.9	2.3	5.7	11.0	23.5	42.0	
Img2Loc	SIGIR'24	15.34	39.83	53.59	69.7	82.78	19.78	30.71	41.4	58.11	74.07	
PIGEON	CVPR'24	11.3	36.7	53.8	72.4	85.3	10.4	23.7	40.6	62.2	77.7	
G3	NeurIPS'24	16.65	40.94	55.56	71.24	84.68	23.99	35.89	46.98	64.26	78.15	
Geo-Ranker	NeurIPS'25	18.79	45.05	61.49	76.31	89.29	32.94	43.54	54.32	69.79	82.45	
<i>Retrieval-free Methods</i>												
PlaNet	ECCV'16	8.5	24.8	34.3	48.4	64.6	5.6	14.3	22.2	36.4	55.8	
CPlaNet	ECCV'18	10.2	26.5	34.6	48.6	64.6	7.9	14.8	21.9	36.4	55.5	
ISNs	ECCV'18	10.5	28.0	36.6	49.7	66.0	6.5	16.2	23.8	37.4	55.0	
Translocator	ECCV'22	11.8	31.1	46.7	58.9	80.1	8.4	18.6	27.0	41.1	60.4	
GeoDecoder	ICCV'23	12.8	33.5	45.9	61.0	76.1	10.3	24.4	33.9	50.0	68.7	
GeoCLIP	NeurIPS'23	14.11	34.47	50.65	69.67	83.82	9.59	19.31	32.63	55.00	74.69	
GLOBE	NeurIPS'25	-	40.18	56.19	71.45	-	-	-	-	-	-	
Geo-R(Ours)		18.10	41.53	58.31	75.33	86.42	10.47	22.67	40.04	60.83	75.84	

Table 1: Main results on IM2GPS3K and YFCC4K (higher is better). The best results achieved by retrieval-free methods are highlighted in bold.

the MP16-Pro dataset (Jia et al. 2024) as described in the Methods section. MP16-Pro contains 4.72 million geotagged Flickr images annotated with hierarchical geographic labels, including country, region, city, and street level, providing a strong foundation for multi-level geographic reasoning. However, it also suffers from missing intermediate labels, inconsistent formatting, and multilingual place names, which reduce the quality of supervision. To address these issues, we standardize annotations by reverse-resolving GPS coordinates into canonical geographic entities, thereby completing missing labels and unifying diverse formats. Both datasets are compatible with the input-output formats required by SFT and RL.

Evaluation Benchmarks We evaluate our model on two widely used geolocation benchmarks to assess both fine-grained localization and global generalization. The IM2GPS3K (Hays and Efros 2008) dataset consists of 3,000 manually curated Flickr images, each annotated with precise GPS coordinates. The images capture a wide variety of outdoor scenes—ranging from cityscapes and iconic landmarks to natural landscapes—making it a challenging benchmark for testing location prediction at high spatial resolution. Complementing this, the YFCC4K (Thomee et al. 2016) dataset contains 4,000 geotagged images sampled from the broader YFCC100M corpus. To ensure balanced geographic coverage, the images are evenly distributed across continents and feature visually diverse content, including urban, rural, and natural settings. Compared to IM2GPS3K, YFCC4K places greater emphasis on testing cross-region generalization under globally heterogeneous environments.

Evaluation Metrics We follow standard protocols established in prior works (Vivanco Cepeda, Nayak, and Shah 2023; Zhou et al. 2024; Jia et al. 2024). Specifically, we compute the geodesic distance between the predicted and ground-truth coordinates for each test sample, and report the percentage of predictions that fall within predefined distance thresholds: 1km, 25km, 200km, 750km, and 2500km. This

metric provides a holistic view of both near-exact localization and coarse regional accuracy.

4.2 Baselines

We compare our method against a range of representative baselines, which can be broadly categorized into retrieval-based and non-retrieval-based methods. Retrieval-based methods include [L]kNN (Vo, Jacobs, and Hays 2017), which aggregates coordinates from the top-k nearest images; Translocator (Pramanick et al. 2022b), a dual-branch transformer leveraging image and segmentation inputs; Img2Loc (Zhou et al. 2024), which incorporates retrieved coordinates into a RAG prompt; and PIGEON (Haas et al. 2024), which retrieves over semantic location clusters. In contrast, non-retrieval methods directly perform prediction without reference data. These include PlaNet (Seo et al. 2018b) and CPlaNet (Seo et al. 2018b), which formulate localization as a classification task over geographical cells; ISNs (Muller-Budack, Pustu-Iren, and Ewerth 2018), which fuses partition hierarchies and scene context; GeoDecoder (Clark et al. 2023b), which models hierarchical relationships via cross-attention; and GeoCLIP (Vivanco Cepeda, Nayak, and Shah 2023), which uses CLIP-based vision-language features with GPS embedding but no external image retrieval.

4.3 Implementation Details

We adopt a two-stage training strategy without relying on any retrieval module, and perform training on Qwen2.5-VL-7B-Instruct, a large vision-language model with built-in multi-modal reasoning capability. The model takes both image inputs and structured location prompts, and is trained to generate geographic reasoning chains along with hierarchical labels and final coordinates.

For the SFT Stage, we use a dataset of 500k samples consisting of images, reasoning chains, and coordinate triples. We optimize a joint objective over coordinate regression and

Size	Data	1km	25km	200km	750km	2500km
3B	-	3.4%	15.9%	33.4%	48.4%	61.4%
3B	CoT	3.7%	16.4%	47.5%	48.2%	66.7%
3B	CoR	4.5%	24.1%	44.8%	56.7%	69.6%
7B	-	5.3%	24.3%	42.4%	61.4%	72.9%
7B	CoT	6.3%	26.1%	44.6%	60.6%	71.9%
7B	CoR	7.1%	33.7%	55.5%	73.4%	85.5%
32B	-	10.2%	29.7%	43.1%	68.4%	73.9%
32B	CoT	11.0%	33.7%	50.5%	67.0%	82.5%
32B	CoR	12.3%	35.0%	50.7%	66.7%	81.4%

Table 2: Comparison of geolocation accuracy across different model sizes and prompting strategies: baseline, CoT for Chain-of-Thought prompting, and CoR for Chain-of-Region reasoning. Accuracy is reported at five distance thresholds from 1km to 2500km on the IM2GPS3K benchmark. CoR introduces hierarchical geographic reasoning before final coordinate prediction.

reasoning chain supervision using the AdamW (Loshchilov and Hutter 2017) optimizer with a learning rate of 1×10^{-5} , batch size of 64, and a total of one epoch.

For the RL Stage, we perform geographic reasoning policy optimization using 200k samples. The model is optimized with policy gradients guided by the composite reward signal described in Section 3.2, incorporating both haversine distance and format. All experiments are conducted on a cluster of 8 NVIDIA A100 GPUs.

4.4 Main Results

Our experimental results underscore the effectiveness of combining structured reasoning with reward-guided optimization for image geolocation. As shown in Table 1, our method consistently outperforms all retrieval-free baselines and achieves performance comparable to retrieval-based approaches on the IM2GPS3K and YFCC4K benchmarks. On IM2GPS3K, our model achieves a 1km accuracy of 18.10%, surpassing prior retrieval-free methods such as GeoCLIP (14.11%) and GLOBE, and even approaching or exceeding several retrieval-based methods. At the 2500km level, our accuracy reaches 86.42%, indicating a strong global localization capability. On the YFCC4K dataset, which contains more challenging and diverse images, our approach achieves 10.47% at 1km and 75.84% at 2500km, again outperforming all retrieval-free models and rivaling top retrieval-based systems. These results demonstrate the synergy between interpretable intermediate supervision and RL, highlighting the value of geographic reasoning as a core component in building robust, retrieval-free geolocation agents.

4.5 Ablation Study

To comprehensively analyze the factors that influence geolocation performance, we conduct ablation studies across four dimensions: reasoning strategy, reasoning supervision, data selection, and reinforcement learning. First, in Reasoning with CoR, we compare three prompting strategies—baseline, Chain-of-Thought (CoT), and our proposed

Size	Type	1km	25km	200km	750km	2500km
-	-	4.5%	24.1%	44.8%	56.7%	69.6%
10k	-	5.8%	25.6%	48.3%	67.7%	82.3%
10k	CoR	7.3%	28.1%	48.6%	69.0%	83.5%
100k	-	8.6%	27.8%	47.6%	67.2%	81.5%
100k	CoR	9.2%	29.9%	49.4%	69.2%	82.8%
500k	-	10.4%	30.9%	48.6%	70.5%	83.7%
500k	CoR	12.6%	31.7%	50.2%	70.3%	84.3%

Table 3: Ablation study on the impact of data scale and prompt format using Qwen2.5-VL-3B. "Size" indicates the number of supervised SFT training samples. "Type" refers to the prompting format, where "-" uses a simple location-only prompt and "CoR" employs our proposed Chain-of-Region reasoning structure.

CoR—to evaluate the impact of explicit reasoning guidance. Second, in Training with CoR, we examine how incorporating structured reasoning chains as supervision, under varying data scales, affects localization accuracy. Third, in Diverse Data Selection, we assess the effect of sampling strategies by comparing random sampling with hard-case sampling, focusing on both fine-grained accuracy and generalization. Finally, in Reinforcement Learning, we investigate how reward-guided optimization improves performance under different supervision settings, particularly in handling challenging examples. Together, these studies highlight the critical role of structured reasoning, data composition, and learning strategy in enhancing both the precision and robustness of geolocation models. Due to the high computational cost of reinforcement learning, we conduct ablation studies using only the 3B parameter-scale model.

Reasoning with CoR We evaluate the geolocation capabilities of Qwen2.5-VL models across three parameter scales—3B, 7B, and 32B—under different prompting strategies, including the baseline, CoT, and our proposed CoR. As shown in Table 2, performance consistently improves with both model scale and the introduction of reasoning guidance. CoR significantly outperforms both the baseline and CoT across all distance thresholds. For example, the 7B model with CoR achieves 33.7% at 25km and 85.5% at 2500km, compared to 26.1% and 71.9% with CoT, demonstrating notable gains in both fine-grained and coarse-level localization. Similar improvements are observed with the 32B model. These results indicate that scaling alone is insufficient, and incorporating explicit geographic reasoning through CoR yields substantial benefits, particularly in the mid- to long-range prediction bands from 200km to 2500km.

Training with CoR We investigate how incorporating structured geographic reasoning into supervision affects model performance. Using Qwen2.5-VL-3B, we compare location-only training with our CoR format under varying data scales. As shown in Table 3, training with CoR reasoning label significantly boosts geolocation accuracy across all distance thresholds. For instance, at 1km, accuracy improves from 7.3% to 12.6% when scaling from 10k to 500k

Size	Sample	1km	25km	200km	750km	2500km
-	-	4.5%	24.1%	44.8%	56.7%	69.6%
10k	Rand	7.3%	28.1%	48.6%	69.0%	83.5%
10k	Hard	4.9%	27.1%	47.8%	67.4%	81.1%
100k	Rand	9.2%	29.9%	49.4%	69.2%	82.8%
100k	Hard	6.0%	28.5%	48.9%	68.0%	82.3%

Table 4: Geolocation accuracy of Qwen2.5-VL-3B trained with supervised SFT under varying data sizes and sampling strategies. All experiments adopt the CoR prompt format unless marked with missing entries. “Size” indicates the number of training samples; “Type” denotes the data selection method, including Rand for random sampling and Hard for hard-case mining.

samples, while at 2500km, it rises from 82.8% to 84.3%. Notably, CoR outperforms location-only baselines at each scale, with consistent gains of 0.6–2.0 percentage points. These results show that reasoning chains improve interpretability and directly enhance coordinate prediction, especially with limited data.

Diverse Data Selection As shown in Table 4, across both training sizes, random sampling (Rand) consistently outperforms hard-case sampling (Hard), especially at fine-grained levels such as 1km. For example, under the 100k setting, Rand achieves 9.2% accuracy at 1km, compared to only 6.0% with Hard—yielding a 3.2 percentage point gap. This performance difference is largely attributed to the nature of hard samples, which often include noisy scenes, ambiguous context, or conflicting multimodal cues.

While such examples are useful for stress-testing model robustness, supervised fine-tuning tends to overfit these difficult instances, as it treats all ground-truth labels as equally reliable and lacks uncertainty modeling. In contrast, random sampling covers a broader and more diverse range of geographic regions and scene types, enabling the model to learn more robust and transferable spatial features.

Reinforcement Learning We further investigate the role of RL in optimizing geolocation performance under different supervision conditions. As shown in Table 5, RL brings consistent improvements, particularly when applied to hard-case data. For instance, under low-resource SFT (10k), applying RL on hard samples improves 1km accuracy from 7.3% to 8.6%, outperforming RL on random samples (6.7%). This suggests that reward-guided optimization better exploits complex examples that are challenging for conventional supervised learning. At larger SFT scales (500k), RL continues to improve performance. Notably, hard-sample RL reaches 14.8% at 1km and 83.8% at 2500km, outperforming both the SFT-only baseline and RL with random data. The gains are especially pronounced in fine-grained localization. These results demonstrate that while random samples contribute to stable SFT training, hard samples become more valuable in RL settings, where reward signals help extract meaningful gradients and mitigate overfitting—ultimately improving generalization to complex, real-world geographic scenarios.

Methods	Sample	1km	25km	200km	750km	2500km
<i>Without Chain of Region</i>						
SFT-10k	-	5.8%	25.6%	48.3%	67.7%	82.3%
+RL	Rand 10k	7.0%	27.6%	41.8%	65.5%	80.6%
+RL	Hard 10k	7.8%	28.6%	52.7%	66.9%	80.7%
<i>With Chain of Region</i>						
SFT-10k	-	7.3%	28.1%	48.6%	69.0%	83.5%
+RL	Rand 10k	6.7%	24.3%	42.5%	61.0%	74.9%
+RL	Hard 10k	8.6%	28.7%	45.7%	69.0%	85.4%
<i>With Chain of Region</i>						
SFT-500k	-	12.6%	31.7%	50.2%	70.3%	84.3%
+RL	Rand 10k	11.3%	28.9%	49.6%	68.7%	79.3%
+RL	Hard 10k	11.1%	31.6%	50.3%	66.2%	78.3%
<i>With Chain of Region</i>						
SFT-500k	-	12.6%	31.7%	50.2%	70.3%	84.3%
+RL	Rand 200k	13.3%	32.4%	51.6%	71.3%	82.3%
+RL	Hard 200k	14.8%	36.3%	54.6%	72.7%	83.8%

Table 5: Evaluation of Qwen2.5-VL-3B under RL with different SFT scales and reward strategies. “SFT-10k/500k” indicates the number of samples used for SFT. “Rand” and “Hard” refer to randomly sampled or hard-case data used in RL. Results demonstrate the effect of SFT and reward-guided RL across multiple geodesic thresholds.

4.6 Result Analysis

Experimental results show that the CoR prompting strategy improves coordinate prediction by breaking down geolocation into structured, hierarchical reasoning steps, thereby aligning the generation process with the model’s internal representations and reasoning mechanisms. The use of structured reasoning data during training further reinforces this capability. However, SFT remains insensitive to coordinate-level errors, making it difficult to optimize localization accuracy precisely (Chu et al. 2025; Shen et al. 2025). With the introduction of RL, the model can directly optimize against geodesic distance, leading to significant improvements in precision—particularly in complex or geographically ambiguous regions.

5 Conclusion

In this paper, we introduced Geo-R, a retrieval-free and reasoning-driven framework for global image geolocalization that combines structured geographic reasoning with reinforcement learning based on verifiable, spatially grounded rewards. Our approach integrates a scalable Chain-of-Region paradigm for interpretable multi-level inference with reward-guided optimization that directly targets geographic plausibility. The results demonstrate that large language model reasoning, without any reliance on external retrieval or synthetic teacher supervision, can deliver competitive or superior localization accuracy, interpretability, and cross-domain generalization. Comprehensive experiments on standard benchmarks validate the effectiveness and robustness of Geo-R, underscoring the potential of reasoning-centric methods for building scalable and general-purpose geographic agents. We hope this work encourages further research into interpretable and verifiable multimodal reasoning, as well as new applications at the intersection of vision, language, and geospatial artificial intelligence.

References

Bai, S.; Chen, K.; Liu, X.; Wang, J.; Ge, W.; Song, S.; Dang, K.; Wang, P.; Wang, S.; Tang, J.; Zhong, H.; Zhu, Y.; Yang, M.; Li, Z.; Wan, J.; Wang, P.; Ding, W.; Fu, Z.; Xu, Y.; Ye, J.; Zhang, X.; Xie, T.; Cheng, Z.; Zhang, H.; Yang, Z.; Xu, H.; and Lin, J. 2025. Qwen2.5-VL Technical Report. *arXiv preprint arXiv:2502.13923*.

Chen, L.; Li, J.; Dong, X.; Zhang, P.; He, C.; Wang, J.; Zhao, F.; and Lin, D. 2023. ShareGPT4V: Improving Large Multi-Modal Models with Better Captions. *arXiv preprint arXiv:2311.12793*.

Chen, L.; Li, L.; Zhao, H.; Song, Y.; and Vinci. 2025. R1-V: Reinforcing Super Generalization Ability in Vision-Language Models with Less Than \$3. <https://github.com/Deep-Agent/R1-V>. Accessed: 2025-02-02.

Chu, T.; Zhai, Y.; Yang, J.; Tong, S.; Xie, S.; Schuurmans, D.; Le, Q. V.; Levine, S.; and Ma, Y. 2025. Sft memorizes, rl generalizes: A comparative study of foundation model post-training. *arXiv preprint arXiv:2501.17161*.

Clark, B.; Kerrigan, A.; Kulkarni, P. P.; Cepeda, V. V.; and Shah, M. 2023a. Where We Are and What We're Looking At: Query-Based Worldwide Image Geo-Localization Using Hierarchies and Scenes. In *Proceedings of the IEEE/CVF Conference on Computer Vision and Pattern Recognition*, 23182–23190.

Clark, B.; Kerrigan, A.; Kulkarni, P. P.; Cepeda, V. V.; and Shah, M. 2023b. Where we are and what we're looking at: Query based worldwide image geo-localization using hierarchies and scenes. In *Proceedings of the IEEE/CVF Conference on Computer Vision and Pattern Recognition*, 23182–23190.

Deng, H.; Zou, D.; Ma, R.; Luo, H.; Cao, Y.; and Kang, Y. 2025. Boosting the Generalization and Reasoning of Vision Language Models with Curriculum Reinforcement Learning. *arXiv preprint arXiv:2503.07065*.

DeSouza, G. N.; and Kak, A. C. 2002. Vision for mobile robot navigation: A survey. *IEEE transactions on pattern analysis and machine intelligence*, 24(2): 237–267.

Firmansyah, H. B.; Fernandez-Marquez, J. L.; Mulayim, M. O.; Gomes, J.; Ribeiro, J.; and Lorini, V. 2024. Empowering Crisis Response Efforts: A Novel Approach to Geolocating Social Media Images for Enhanced Situational Awareness. In *Proceedings of the International ISCRAM Conference*.

Guo, D.; Yang, D.; Zhang, H.; Song, J.; Zhang, R.; Xu, R.; Zhu, Q.; Ma, S.; Wang, P.; Bi, X.; et al. 2025. Deepseek-r1: Incentivizing reasoning capability in llms via reinforcement learning. *arXiv preprint arXiv:2501.12948*.

Haas, L.; Alberti, S.; and Skreta, M. 2023. Learning generalized zero-shot learners for open-domain image geolocalization. *arXiv preprint arXiv:2302.00275*.

Haas, L.; Skreta, M.; Alberti, S.; and Finn, C. 2024. Pigeon: Predicting image geolocations. In *Proceedings of the IEEE/CVF Conference on Computer Vision and Pattern Recognition*, 12893–12902.

Hao, X.; Chen, W.; Zou, X.; and Liang, Y. 2025. Nature makes no leaps: Building continuous location embeddings with satellite imagery from the web. In *Proceedings of the ACM on Web Conference 2025*, 2799–2812.

Hays, J.; and Efros, A. A. 2008. Im2gps: estimating geographic information from a single image. In *2008 ieee conference on computer vision and pattern recognition*, 1–8. IEEE.

Jia, P.; Liu, Y.; Li, X.; Zhao, X.; Wang, Y.; Du, Y.; Han, X.; Wei, X.; Wang, S.; and Yin, D. 2024. G3: an effective and adaptive framework for worldwide geolocalization using large multi-modality models. *Advances in Neural Information Processing Systems*, 37: 53198–53221.

Koh, J. Y.; Salakhutdinov, R.; and Fried, D. 2023. Grounding language models to images for multimodal inputs and outputs. In *International Conference on Machine Learning*, 17283–17300. PMLR.

Kool, W.; van Hoof, H.; and Welling, M. 2019. Buy 4 reinforce samples, get a baseline for free!

Körting, T. S.; Fonseca, L. M. G.; and Câmara, G. 2013. GeoDMA—Geographic data mining analyst. *Computers & Geosciences*, 57: 133–145.

Liang, Y.; Ke, S.; Zhang, J.; Yi, X.; and Zheng, Y. 2018. Geoman: Multi-level attention networks for geo-sensory time series prediction. In *IJCAI*, volume 2018, 3428–3434.

Liu, X.; Hu, J.; Li, Y.; Diao, S.; Liang, Y.; Hooi, B.; and Zimmermann, R. 2024. Unitime: A language-empowered unified model for cross-domain time series forecasting. In *Proceedings of the ACM Web Conference 2024*, 4095–4106.

Liu, Z.; Sun, Z.; Zang, Y.; Dong, X.; Cao, Y.; Duan, H.; Lin, D.; and Wang, J. 2025. Visual-rft: Visual reinforcement fine-tuning. *arXiv preprint arXiv:2503.01785*.

Loshchilov, I.; and Hutter, F. 2017. Decoupled weight decay regularization. *arXiv preprint arXiv:1711.05101*.

Lu, P.; Bansal, H.; Xia, T.; Liu, J.; Li, C.; Hajishirzi, H.; Cheng, H.; Chang, K.-W.; Galley, M.; and Gao, J. 2023. Mathvista: Evaluating mathematical reasoning of foundation models in visual contexts. *arXiv preprint arXiv:2310.02255*.

Muller-Budack, E.; Pustu-Iren, K.; and Ewerth, R. 2018. Geolocation estimation of photos using a hierarchical model and scene classification. In *Proceedings of the European conference on computer vision (ECCV)*, 563–579.

Müller-Budack, E.; Pustu-Iren, K.; and Ewerth, R. 2018. Geolocation estimation of photos using a hierarchical model and scene classification. In *Proceedings of the European Conference on Computer Vision*, 563–579.

Pan, Z.; Liang, Y.; Wang, W.; Yu, Y.; Zheng, Y.; and Zhang, J. 2019. Urban traffic prediction from spatio-temporal data using deep meta learning. In *Proceedings of the 25th ACM SIGKDD international conference on knowledge discovery & data mining*, 1720–1730.

Peng, Y.; Zhang, G.; Zhang, M.; You, Z.; Liu, J.; Zhu, Q.; Yang, K.; Xu, X.; Geng, X.; and Yang, X. 2025. LMM-R1: Empowering 3B LMMs with Strong Reasoning Abilities Through Two-Stage Rule-Based RL. *arXiv preprint arXiv:2503.07536*.

Pramanick, S.; Nowara, E. M.; Gleason, J.; Castillo, C. D.; and Chellappa, R. 2022a. Where in the world is this image? transformer-based geo-localization in the wild. In *Proceedings of the European Conference on Computer Vision*, 196–215.

Pramanick, S.; Nowara, E. M.; Gleason, J.; Castillo, C. D.; and Chellappa, R. 2022b. Where in the world is this image? transformer-based geo-localization in the wild. In *European Conference on Computer Vision*, 196–215. Springer.

Seo, P. H.; Weyand, T.; Sim, J.; and Han, B. 2018a. Cplanet: Enhancing image geolocalization by combinatorial partitioning of maps. In *Proceedings of the European Conference on Computer Vision*, 536–551.

Seo, P. H.; Weyand, T.; Sim, J.; and Han, B. 2018b. Cplanet: Enhancing image geolocalization by combinatorial partitioning of maps. In *Proceedings of the European Conference on Computer Vision (ECCV)*, 536–551.

Shao, Z.; Wang, P.; Zhu, Q.; Xu, R.; Song, J.; Bi, X.; Zhang, H.; Zhang, M.; Li, Y.; Wu, Y.; et al. 2024. Deepseekmath: Pushing the limits of mathematical reasoning in open language models. *arXiv preprint arXiv:2402.03300*.

Shen, H.; Liu, P.; Li, J.; Fang, C.; Ma, Y.; Liao, J.; Shen, Q.; Zhang, Z.; Zhao, K.; Zhang, Q.; et al. 2025. Vlm-r1: A stable and generalizable r1-style large vision-language model. *arXiv preprint arXiv:2504.07615*.

Sinnott, R. W. 1984. Virtues of the Haversine. *Sky and telescope*, 68(2): 158.

Thomee, B.; Shamma, D. A.; Friedland, G.; Elizalde, B.; Ni, K.; Poland, D.; Borth, D.; and Li, L.-J. 2016. Yfcc100m: The new data in multimedia research. *Communications of the ACM*, 59(2): 64–73.

Vivanco Cepeda, V.; Nayak, G. K.; and Shah, M. 2023. Geoclip: Clip-inspired alignment between locations and images for effective worldwide geo-localization. *Advances in Neural Information Processing Systems*, 36: 8690–8701.

Vo, N.; Jacobs, N.; and Hays, J. 2017. Revisiting im2gps in the deep learning era. In *Proceedings of the IEEE international conference on computer vision*, 2621–2630.

Wang, B.; Wu, B.; Li, W.; Fang, M.; Liang, Y.; Huang, Z.; Wang, H.; Huang, J.; Chen, L.; Chu, W.; et al. 2025a. Infinity Parser: Layout Aware Reinforcement Learning for Scanned Document Parsing. *arXiv preprint arXiv:2506.03197*.

Wang, H.; Qu, C.; Huang, Z.; Chu, W.; Lin, F.; and Chen, W. 2025b. Vl-rethinker: Incentivizing self-reflection of vision-language models with reinforcement learning. *arXiv preprint arXiv:2504.08837*.

Wang, X.; Xu, R.; Cui, Z.; Wan, Z.; and Zhang, Y. 2023. Fine-grained cross-view geo-localization using a correlation-aware homography estimator. *Advances in Neural Information Processing Systems*, 36: 5301–5319.

Weyand, T.; Kostrikov, I.; and Philbin, J. 2016. Planet-photo geolocation with convolutional neural networks. In *Proceedings of the European Conference on Computer Vision*, 37–55.

Wu, B.; Li, Y.; Wei, Y.; Fang, M.; and Chen, L. 2024. Foundations and recent trends in multimodal mobile agents: A survey. *arXiv preprint arXiv:2411.02006*.

Xia, Z.; and Alahi, A. 2025. FG^2 : Fine-Grained Cross-View Localization by Fine-Grained Feature Matching. *arXiv preprint arXiv:2503.18725*.

Yan, Y.; Wen, H.; Zhong, S.; Chen, W.; Chen, H.; Wen, Q.; Zimmermann, R.; and Liang, Y. 2024. Urbanclip: Learning text-enhanced urban region profiling with contrastive language-image pretraining from the web. In *Proceedings of the ACM Web Conference 2024*, 4006–4017.

Yang, H.; Lu, X.; and Zhu, Y. 2021. Cross-view geo-localization with layer-to-layer transformer. *Advances in Neural Information Processing Systems*, 34: 29009–29020.

Yang, Y.; He, X.; Pan, H.; Jiang, X.; Deng, Y.; Yang, X.; Lu, H.; Yin, D.; Rao, F.; Zhu, M.; et al. 2025. R1-Onevision: Advancing Generalized Multimodal Reasoning through Cross-Modal Formalization. *arXiv preprint arXiv:2503.10615*.

Ye, Y.; Richards, D.; Lu, Y.; Song, X.; Zhuang, Y.; Zeng, W.; and Zhong, T. 2019a. Measuring daily accessed street greenery: A human-scale approach for informing better urban planning practices. *Landscape and Urban Planning*, 191: 103434.

Ye, Y.; Zeng, W.; Shen, Q.; Zhang, X.; and Lu, Y. 2019b. The visual quality of streets: A human-centred continuous measurement based on machine learning algorithms and street view images. *Environment and Planning B: Urban Analytics and City Science*, 46(8): 1439–1457.

Yeh, A. G. 1999. Urban planning and GIS. *Geographical information systems*, 2(877-888): 1.

Zhou, H.; Li, X.; Wang, R.; Cheng, M.; Zhou, T.; and Hsieh, C.-J. 2025. R1-Zero’s “Aha Moment” in Visual Reasoning on a 2B Non-SFT Model. *arXiv preprint arXiv:2503.05132*.

Zhou, Z.; Zhang, J.; Guan, Z.; Hu, M.; Lao, N.; Mu, L.; Li, S.; and Mai, G. 2024. Img2Loc: Revisiting image geolocalization using multi-modality foundation models and image-based retrieval-augmented generation. In *Proceedings of the 47th International ACM SIGIR Conference on Research and Development in Information Retrieval*, 2749–2754.

Zhu, S.; Shah, M.; and Chen, C. 2022. Transgeo: Transformer is all you need for cross-view image geo-localization. In *Proceedings of the IEEE/CVF Conference on Computer Vision and Pattern Recognition*, 1162–1171.